2020

A multipurpose desalination, cooling, and air-conditioning system powered by waste heat recovery from submarine diesel exhaust fumes and cooling water

Abdellah Shafieian
Edith Cowan University, a.shafieiandastjerdi@ecu.edu.au

Mehdi Khiadani
Edith Cowan University, m.khiadani@ecu.edu.au

10.1016/j.csite.2020.100702
Shafieian, A., & Khiadani, M. (2020). A multipurpose desalination, cooling, and air-conditioning system powered by waste heat recovery from diesel exhaust fumes and cooling water. *Case Studies in Thermal Engineering*, *21*, Article 100702. https://doi.org/10.1016/j.csite.2020.100702

Case Studies in Thermal Engineering 21 (2020) 100702

Contents lists available at ScienceDirect

Case Studies in Thermal Engineering

journal homepage: http://www.elsevier.com/locate/csite

A multipurpose desalination, cooling, and air-conditioning system powered by waste heat recovery from diesel exhaust fumes and cooling water

Abdellah Shafieian, Mehdi Khiadani *

School of Engineering, Edith Cowan University, 270 Joondalup Drive, Joondalup, Perth, WA, 6027, Australia

HIGHLIGHTS

- A novel desalination, cooling, and air-conditioning system for energy recovery.
- Freshwater productivity is more sensitive to temperature than mass flow rate.
- The coefficient of performance for the cooling system is 0.88.
- The achieved refrigeration power range is130–190 kW.
- Advantages like operation durability increase and fuel consumption decrease.

ARTICLE INFO

Keywords:
Membrane distillation
Absorption chiller
Desalination
Submarine engines

ABSTRACT

The role of cooling and air-conditioning systems in submarines is assessed as indispensable, and a reliable water supply is essential for both crew and equipment. At the same time, the large amounts of high-temperature exhaust fumes discharged from submarine engines provide an excellent opportunity to recover and apply this waste energy in required applications. This paper introduces a novel multipurpose desalination, cooling, and air-conditioning system to recover waste heat from both the exhaust fumes and the cooling water of submarine engines. The whole system is mathematically modelled and analysed based on the actual thermo-physical parameters of the engine's exhaust fumes. The analysis indicates that at cooling water flow rate of 0.25 kg/s and diesel exhaust mass ratio (X) of 0.25, the mass flux through the membrane in the desalination unit reaches 8.3 kg/m^{2}h. Whereas for the same cooling water flow rate, the mass flux increases by 2 kg/m^{2}h as X increases from 0.25 to 0.3. The results also show that a 160 kW cooling power is only achievable when X varies between 0.8 and 0.95 and the refrigerant mass flow rate is in the range of 0.27 kg/s to 0.34 kg/s.

1. Introduction

Submarines use their diesel engines to recharge the batteries that propel them underwater and also support some of their other systems. Hot exhaust gases are directed overboard by exhaust discharge systems, while water is used to cool down the engine. According to verified standards, a large amount of combustion energy in submarine engines remains unused and wasted. Depending on the submarine specifications, the exhaust gases' temperature may reach 650 °C, at flow rates between 6116 m^3/h and 14,611 m^3/h

* Corresponding author.
E-mail addresses: a.shafieiandastjerdi@ecu.edu.au (A. Shafieian), m.khiadani@ecu.edu.au (M. Khiadani).

https://doi.org/10.1016/j.csite.2020.100702
Received 20 May 2020; Received in revised form 21 June 2020; Accepted 22 June 2020
Available online 26 June 2020

Nomenclature

A	Area (m^2)
C_p	molar heat capacity (J/mol.K)
C_m	Membrane-specific Mass transfer coefficient (kg/m^2sPa)
cv	Control volume
D	Diffusion coefficient
d_e	Vapour and air collision diameter
d_h	hydraulic diameter (m)
E	Energy rate (W)
f	Feed
H_v	vaporization enthalpy (J/kg)
h	Convective heat transfer coefficient (W/m^2K)/enthalpy (kJ/kg)
i	inlet
J	Transmembrane water flux (kg/m^2s)
k_m	Membrane module thermal conductivity (W/m.K)
K_g	Air thermal conductivity inside the pores (W/m.K)
k_b	Boltzmann constant ($1.380622^* 10^{-23}$ J/K)
k	Film mass transfer coefficient (m/s)
L	Length (m)
M	Molecular weight (kg/mol)
m_o	outlet mass flow rate (kg/s)
m_i	inlet mass flow rate (kg/s)
m	Membrane surface/mass flow rate (kg/s)
Nu	Nusselt number
n	Step/section number
o	Outlet
p	Permeate
Pr	Prandtl number
P_a	entrapped air pressure (Pa)
P_v	vapour pressure at given salinity (Pa)
$P_{m,p}$	vapour pressure at cold membrane surface (Pa)
$P_{m,f}$	vapour pressure at hot membrane surface (Pa)
P	Pressure (Pa)/average pressure inside the membrane pores (Pa)
t	Time (s)
P	Average pressure inside the pores of the membrane (Pa)
P_v	Vapour pressure (Pa)
P_a	Air pressure (Pa)
Q_e	evaporator thermal power (kW)
Q_{ex}	exhaust gas thermal power (kW)
Q_{jw}	jacket water thermal power (kW)
Q_n	Heat flux (W/m^2)
Q	Heat transfer rate (KW)
R	Gas constant (J/kg.K)
r	Membrane pore diameter (m)
Re	Reynolds number
S	Salinity
T	Temperature (K)
T_0	constant (221 K)
T_b	bulk temperature (K)
T_c	critical point temperature
t	Time
U	Overall heat transfer coefficient (W/m^2K)
v	Vapour
V	Velocity (m/s)
W	electric power (kW)
w	Water
X	exhaust gas mass ratio
x	molar fraction
x_c	weight fraction of salt in water

Y	Specific enthalpy (J/kg)

Greek Letters

ω	solution concentration
σ	denotes a state on the vapour-pressure curve
δ	Thickness (m)
ρ	Density (kg/m^3)
ε	Porosity
τ	Membrane tortuosity

while the flow rate of the engine cooling water varies between 0.44 kg/s and 0.95 kg/s [1]. This provides a great opportunity to recover and use large amount of wasted energy for required applications.

To date, most of the studies in the field of engines' waste heat recovery have been mainly focused on generating power or optimising heat exchangers [2,3]. For instance, to recover waste heat in truck diesel engines, Xu et al. [4] proposed a comprehensive dynamic heat recovery model aiming to generate power by utilizing an organic Rankine cycle (ORC) system. Finding ORC waste heat recovery as an effective method to reduce fossil fuel consumption of diesel engines, Koppauer et al. [5] attempted to find the optimum conditions of such systems by developing mathematical models and validating their results by experimental measurements.

In a novel design study, a two-step system to recover the waste thermal energy from both the exhaust fume and the coolant water of a diesel engine was proposed [6]. Yang et al. [7] theoretically analysed the performance of a dual loop ORC for heat recovery from compressed natural gas engines to find the optimum working fluid to be applied in ORCs to reach the minimum economic cost where the high temperature loop was powered by exhaust fumes and the low temperature loop was heated by both jacket water and the condenser section of the high temperature loop.

Chintala et al. [8] comprehensively reviewed the application of ORCs in waste heat recovery from exhaust fume, cooling water and intake air of different engines. In a similar study focused on vehicle engines with different operating conditions, Lion et al. [9] gave an overview of ORC systems to recover waste heat from exhaust fume, engine cooling system, intake air system, and oil circuit.

Studies in the field of engines' waste heat recovery have not been limited to power generation and some researchers have proposed novel systems with various applications. For instance, with the aim of reducing fossil fuel consumption and environmental pollution, Lan et al. [10] proposed the application of thermoelectric generators in vehicle engines by developing a dynamic model and also setting up a small experimental rig. Goyal et al. [11] conducted an experimental investigation on a small-scale absorption chiller powered by recovered waste heat of a diesel generator.

In recent years, noticeable attention has also been paid towards waste heat recovery of marine engines due to their high capacity, high exhaust temperatures and flow rates, fossil fuel challenges, and environmental and marine pollution. Similar to other types of engines, power generation has been the main purpose of the proposed heat recovery systems for marine diesel engines. Liu et al. [12] proposed a cogeneration system for cooling and electricity production which was driven by waste heat recovery from marine engines. The waste heat from both exhaust fumes and cooling water was recovered in their system and used in an organic Rankine cycle and an absorption refrigeration cycle. Steam Rankine and organic Rankine cycles were combined by Liu et al. [13] to form a novel system aimed to recover waste heat from marine engines. Around 4.5% improvement was observed in the thermal efficiency of the engine using the proposed system. In a review paper, Lion et al. [14] presented the technologies and their potentials for waste heat recovery from marine combustion engines and concluded that Organic Rankine Cycles ate the most popular and studied systems.

Liang et al. [15] applied the recovered heat from an internal combustion engine to run a novel refrigeration system comprising transcritical and supercritical CO_2 refrigeration cycles. In a similar study, Mohammed et al. [16] focused on a supercritical Organic Rankine Cycle for waste heat recovery from marine diesel engines. Different configurations for waste energy recovery from marine dual engines were investigated by Su et al. [17] who investigated the optimal matching type by theoretically focusing on the performance of subsystems. Zhu et al. [18] reviewed the most efficient cycles used for electricity generation by waste heat recovery from marine engines and concluded that 4–15% of fuel can be saved using the recovery system.

Eddine et al. [19] investigated the application of two types of thermoelectric generators; Silicon–Germanium and Bismuth-Telluride; in waste heat recovery from marine engines through theoretical and experimental studies. The fact that more than half of the combustion energy is often wasted in fishing vessels engines has been the main motivation for many studies. Xiangguo et al. [20] reviewed the publications about the refrigeration systems powered by exhaust fume waste heat recovery from fishing vessels engines.

With the aim of enhancing the thermal efficiency of marine engines, Ouyang et al. [21] designed and proposed a desulfurization, desalination, and refrigeration system to be driven by the waste heat recovery of the engines. The proposed system was concluded to be reasonably utilisable in different forms of marine engines. Hatami et al. [22] developed a CFD model and investigated different types of finned tube heat exchangers used for waste heat recovery of combustion engines. The focal point of their study was investigating the sensitivity of the amount of the recovered heat to the size and quantity of the fins under different engine loads. Jaber et al. [23] focused on heat recovery from exhaust gases of a generator by proposing a hybrid system for water heating and electricity production.

Among different types of marine diesel engines, submarine engine produces significant amount of exhaust gas with high temperature. Despite the great potential, heat recovery from submarine diesel engines remains inattentive and very limited studies have been reported in this field. Daghigh and Shafieian [24] proposed a combined cooling, heating and power (CHP) system to reuse waste heat from submarine engines.

At the same time, submarine designers usually face two important challenges including high moisture and high temperature inside the cabin. Interior space of a submarine is a closed environment with specified numbers of crew and equipment and a considerable amount of heat is transferred from the seawater to a submarine. In addition, hot engines, electrical batteries, stoves, lights, and crews are other sources of continuous heat production inside submarines. Also, the amount of moisture in the air inside a submarine increase permanently because of storage batteries, kitchen activities, and crew leading to low air quality.

Besides the difficulties with low air quality such as respiration and moisture condensation on equipment, the increase of temperature will also cause functional problems on sensitive electrical devices which put them at risk. Consequently, the role of cooling and air-conditioning systems in submarines is significant. Also, access to fresh water is essential for all submarines, therefore a built-in distillation plant guarantees sustained accessibility to high quality fresh water to be used for cooling electronic equipment and for crew consumption [29]. Overall, the large quantity of discharged exhaust gas with high temperature in submarine engines provides a bedrock for further studies to apply this source of energy in the abovementioned applications.

In this study, a novel combined desalination, cooling, and air conditioning system is proposed and mathematically modelled and analysed based on the actual thermo-physical parameters of exhausted fumes of submarine diesel engine. The main originality of this paper lies in (i) waste heat recovery from both exhaust fume and cooling water of the engine and using it to drive (ii) a built-in direct contact membrane-based desalination plant to produce enough fresh water for different applications (e.g., drinking and cooling purposes) and (iii) to drive a mixed effect absorption cooling and air-conditioning system. The outcomes of this study can lead to fuel economy improvement of submarines, CO_2 reduction, and independency to potable water resources. Submarines using this system will not have to carry large volume of fresh water, instead, can be equipped with smaller fuel storage tanks. This will significantly decrease their weight and required driving power, hence, allowing them to stay and operate underwater for longer time.

2. System description

Fig. 1 presents the schematic diagram of the proposed system for the recovery of thermal energy from a submersible diesel engine. A typical heating system consisting of a heat exchanger (HU), is applied to extract a fraction of heat from the diesel exhaust gases and transfer it to cool seawater. The output hot seawater is utilised in a direct contact membrane-based desalination unit (DU) which applies the recovered heat to produce fresh water. The outlet exhaust gases from the heat exchanger (HU), which still have high temperature, move towards a mixed effect absorption chiller unit (ACU). Along with exhaust gases and in a separate loop, hot jacket water is also directed towards the ACU in which heat from both diesel exhaust gases and engine cooling water is recovered.

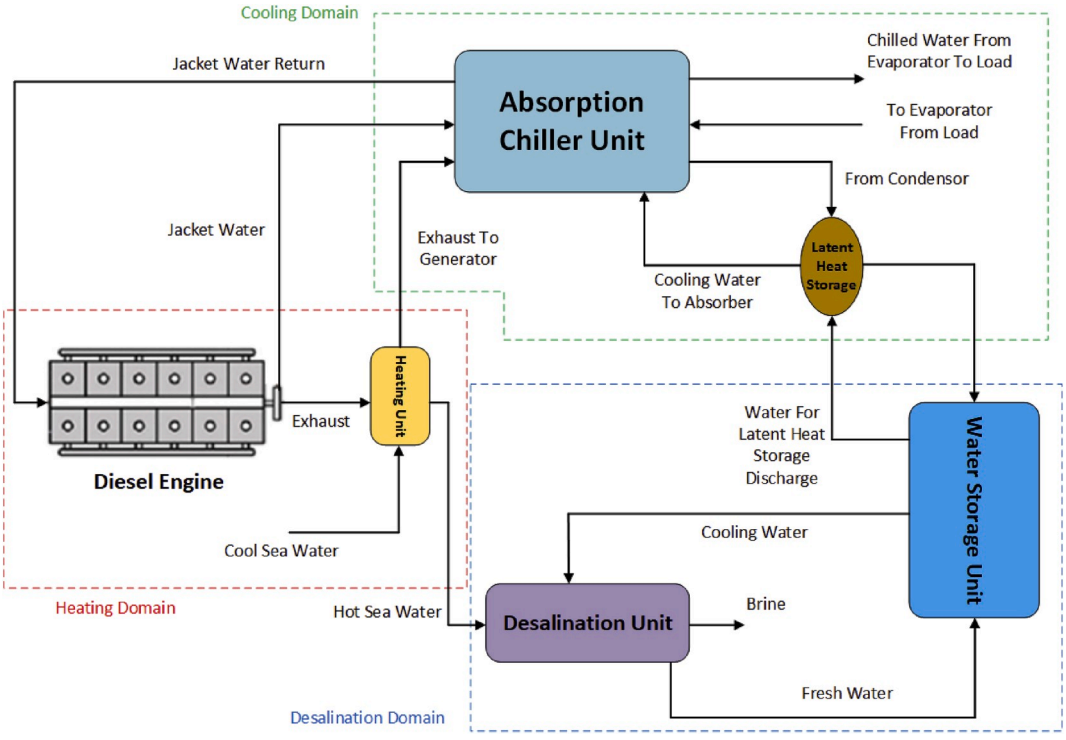

Fig. 1. Schematic diagram of the proposed system for combined desalination, cooling, and air conditioning.

2.1. Mixed effect absorption cooling unit

Fig. 2 presents the schematic diagram of the mixed effect absorption cooling cycle which consists of five main sections: high pressure generator (HPG), condenser, low pressure generator (LPG), evaporator, and absorber.

The main difference between double effect and mixed effect absorption chillers lies in their LPG configuration where the LPG of the mixed effect unit is separated into two sections. So, this system has three generators (i.e. HPG, LPG1 (upper section), LPG2 (lower section)). The jacket water used for cooling engine flows inside an internal loop and, hence, cannot be integrated with ACU directly. Therefore, a heat exchanger (HE) is considered to transfer heat from jacket water to another water loop. The lithium-bromide solution is shown to have the best performance when it is used in systems similar to the proposed unit in Fig. 2 [25]. Consequently, it was selected as the refrigeration working fluid in the simulated system.

Inside heat exchanger 1 (HE1), the dilute solution 1 (water-lithium bromide) from absorber is preheated by the concentrated solution 3 from LGP2. The preheated dilute solution 2 is then divided into two streams. The first stream moves towards LPG1 and receives heat from the hot water comes from HE. So, some of the refrigerant, inside the solution vaporizes turning the status of the solution into semi-dilute solution 10. The semi-dilute solution 10 then moves towards LPG2 for further desorption.

The second stream of dilute solution 2 passes through heat exchanger 2 (HE2) for further preheating. The preheated dilute solution 5 moves towards HPG and receives heat from the hot exhaust gases. Some of the refrigerant, inside the solution, vaporizes (8) and moves towards LPG2 turning dilute solution 5 into semi-dilute solution 6. After heat recovery in HE2, semi-dilute solution 7 moves towards LPG2 and mixes with semi-dilute solution 10 comes from LPG1. The vapour 8 condenses in LPG2 provides the required heat for vaporization of some refrigerant turning mixed semi-dilute solution into concentrated solution 3. The concentrated solution 3 then passes HE1 and moves towards absorber for repeating the absorption process.

The generated refrigerant vapour inside both LPG1 and LPG2 enters condenser section transfers its heat to the cooling water (which comes from latent heat storage (LHS) and passes through the absorber) and condenses. The refrigerant liquid then joins the condensed refrigerant which comes from the LPG2. All absorption chillers need cooling water loop which is supplied by using cooling towers in common applications. However, taking into account the space, weight, and technical justifications, it is not feasible to use a cooling tower inside a submarine. Therefore, LHS is considered in the ACU to provide the required cooling water. As shown in Fig. 1, water circulates inside a closed loop transferring the absorbed heat from ACU to the phase change material inside LHS (Charging process). To cool the LHS, water from storage unit is used (Discharging process).

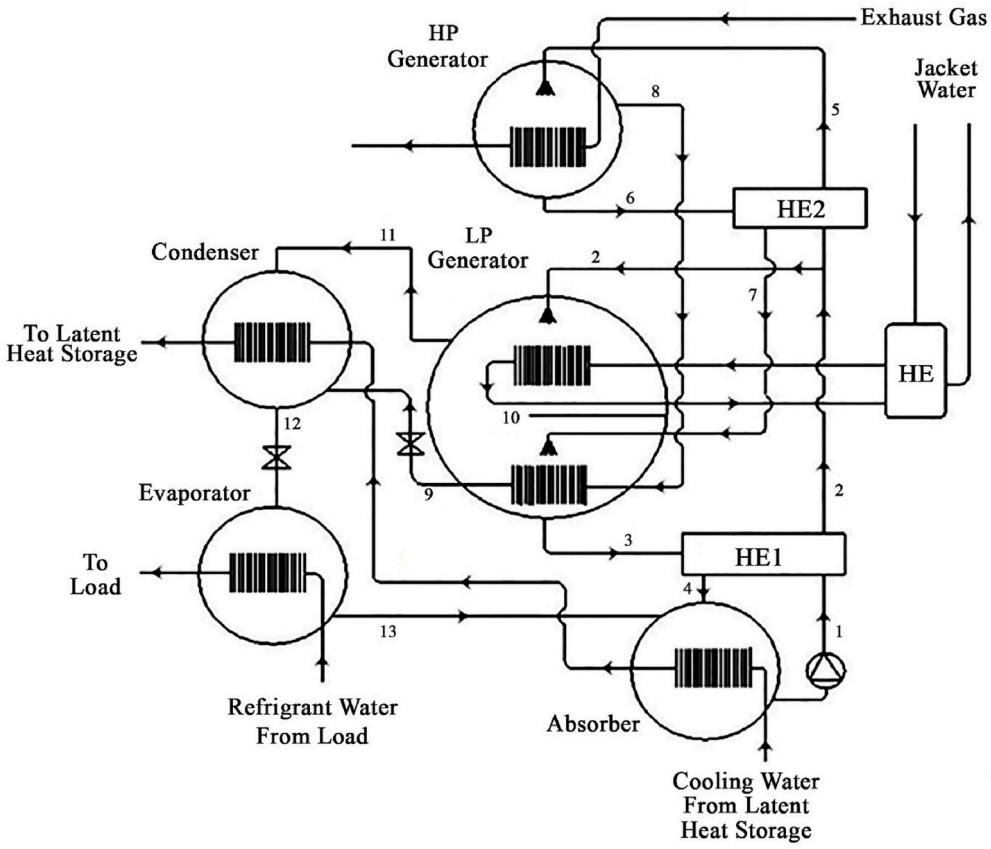

Fig. 2. Schematic of the mixed effect cooling unit.

The combined solution then passes through the pressure reduction valve before entering the evaporator. In this section, refrigerant evaporates and reduces the temperature of water by absorbing its heat. The chilled water then moves towards the load for cooling and air conditioning. The refrigerant vapour enters the absorber, transfers its heat to the cooling water which comes from latent heat storage and turns into liquid again.

2.2. Membrane distillation process

Membrane distillation modules involve two channels separated by micro porous membrane [26]. Vapour transfers from the hot side (or feed channel) to the cold side (or permeate channel) due to the existing vapour pressure difference [27]. In direct contact membrane distillation systems, both hot and cold streams have direct contact with both the hot and the cold surfaces of the membrane module [28].

Waste exhaust gases are applied in HU to raise the temperature of seawater and the resulting outlet hot seawater flows inside the membrane's feed channel to provide the required heat for evaporation at the feed side of the membrane. Once the evaporated water in feed channel passes through the membrane, it condenses to liquid with the condensation heat being absorbed by the cold water at the permeate side of the membrane (product channel). The cold water inside the cold channel is supplied by a permeate tank connected to the DU in which fresh water is stored. The temperatures of the membrane sides differ from those of the mean flow stream inside the cold and hot channels. This is mainly due to the constant evaporation and condensation and the temperature gradient near the membrane surface.

Space justification is an important parameter in a submarine because in contrast to weight, submarines are critically limited to space. Almost all of the components of the proposed system, including absorption chiller, water storage unit, and heating units, already exist inside a submarine and are powered by conventional resources (such as electricity from battery bank) [29]. The desalination unit comprises several DCMD modules which are compact and do not require a significant space. Therefore, combining a heat recovery system with these units does not require a significant extra space. Overall, the combined heat recovery system is both weight and space justified.

3. Mathematical model

For the purpose of performing thermal analysis, determining the diesel exhaust characteristics (e.g., heat capacity, viscosity, etc.) is indispensable before calculating the key parameters such as Reynolds and Nusselt numbers. Taking into account that the diesel exhaust fume mainly consists of N_2, H_2O, O_2 and CO_2, their characteristics are extracted from REFPROP software [34]. It is worth noting that these components have different mass ratios in the combustion process which should be considered in calculating the properties of the exhaust fumes.

3.1. Membrane desalination system

To calculate the temperature and salinity changes along the module, it is discretised into smaller sections. The sections are perpendicular to the direction of feed and permeate streams. The energy as well as mass balance equations have to be solved for all the sections of the membrane. Inlet boundary conditions of each section are the outlet parameters of previous section. The discretisation should be proceeded from the inlet of hot channel towards its outlet for both streams. As a result, the subscript n, which represents the inlet parameters of the hot stream sections, is considered as the outlet parameters of the cold stream sections.

3.1.1. Energy and mass balance equations

Energy transfer by heat and mass in both channels can be determined by considering the following assumptions.

(i) there is no input work.
(ii) constant potential energy across each section.

$$E_{f-n,in} - E_{f-n,out} = \frac{dE_{f-cv}}{dt} \tag{1}$$

$$E_{f-n,in} = E_{f-n,out} \tag{2}$$

$$m_{f,n}\left(Y_{f,n} + \frac{V^2_{f,n}}{2}\right) = m_{f,n+1}\left(Y_{f,n+1} + \frac{V^2_{f,n+1}}{2}\right) + Q_n A_{m,n} \tag{3}$$

$$m_{p,n}\left(Y_{p,n} + \frac{V^2_{p,n}}{2}\right) = m_{p,n+1}\left(Y_{p,n+1} + \frac{V^2_{p,n+1}}{2}\right) + Q_n A_{m,n} \tag{4}$$

Mass flux (J_w) exists in the membrane module, and as a result, the mass flow rate in each section is not equal to the previous section. The mass flow rate of sections in hot and cold channels can be obtained by

$$m_{f,n+1} = m_{f,n} - J_{w,n} A_{m,n} \tag{5}$$

$$m_{p,n+1} = m_{p,n} - J_{w,n}A_{m,n} \tag{6}$$

Solving mentioned equations depend on determination of several parameters including mass transfer through the membrane, heat transfer rate, outlet temperature of hot and cold channels, and membrane surface temperature. Equations presented in the following sections can be applied to calculate the mentioned parameters.

3.1.2. Heat and mass transfer

The temperature difference which exists between two sides of the membrane in a DCMD module results in creation of a vapour pressure gradient force. This results in vapour transfer from the hot channel to the cold channel. There is a linear relationship between the vapour transfer and the vapour pressure difference [30]:

$$J_w = C_m\left[P_v\left(T_{f,m}, S_{f,m}\right) - P_v\left(T_{p,m}, S_{p,m}\right)\right] \tag{7}$$

where C_m (kg/m^{2}sPa) is the MD coefficient and P_v (Pa) represents the vapour pressure at the surfaces of the membrane. The membrane distillation coefficient is determined based on the flow process inside the pores of the membrane module. Temperature and salinity are the two main parameters which affect the thermo-physical characteristics of water. Equations provided by Sharqawy et al. [31] were used to determine the thermo-physical characteristics of water. Mass flux through the membrane is calculated as follows by considering the temperature and salinity at the membrane surfaces as well as heat and mass transfer coefficients.

3.1.2.1. Heat transfer. Three different equations were considered to model the heat transfer processes inside the DCMD module:

(i) Q_f: heat transfer from the feed stream in hot channel to the forming boundary layer near the membrane surface
(ii) Q_m: combination of conduction heat transfers through the membrane and vapour movement through the pores
(iii) Q_p: heat transfer from the permeate boundary layer to the permeate stream in the cold channel [32]:

$$Q_f = h_f\left(T_f - T_{f,m}\right) \tag{8}$$

$$Q_m = h_m\left(T_{f,m} - T_{p,m}\right) + J_w H_v\left(T_{f,m}, S_{f,m}\right) \tag{9}$$

$$Q_p = h_p\left(T_p - T_{p,m}\right) \tag{10}$$

The heat transfer coefficient of the hydrophobic membrane (h_m) can be obtained by:

$$h_m = \frac{k_g\varepsilon + k_m(1-\varepsilon)}{\delta} \tag{11}$$

Based on the steady state assumption:

$$Q_m = Q_f = Q_p = Q \tag{12}$$

The overall heat transfer of the DCMD module is calculated by:

$$Q = U\left(T_f - T_p\right) = \left[\frac{1}{h_f} + \frac{1}{\frac{J_w H_v}{\left(T_{f,m} - T_{p,m}\right)}} + \frac{1}{h_p}\right] \tag{13}$$

3.1.2.2. Mass transfer. The mass balance equation along with the film theory on the hot side boundary layer is applied to specify the salinity of the membrane surface [33]:

$$S_{f,m} = S_f \exp\left(\frac{J_w}{\rho_f K}\right) \tag{14}$$

where K (m/s) in this equation is the film mass transfer coefficient and Sherwood number (Sh) can be used to calculate this parameter [34]:

$$Sh = 0.023 Re^{0.83} Sc^{0.33} \tag{15}$$

$$Sh = \frac{K_s D_h}{D_{w-a}} \tag{16}$$

where D_h is the hydraulic diameter while $D_{w\text{-}a}$ represents the water vapour diffusion coefficient in stagnant air, respectively. Schmidt number in Eq. (15) can be determined by Ref. [35]:

$$Sc = \frac{\mu}{\rho D_{w-a}} \tag{17}$$

The ratio of the transferred molecules mean free path (S) to the pore dimension of the module (d) is called Knudsen number. This parameter acts as a quantitative measurement in specification of flow type.

$$Kn = \frac{S}{d} \tag{18}$$

The average transported molecules free path can be obtained from Ref. [36]:

$$S = \frac{K_b T}{1.44 \pi P d_e^2} \tag{19}$$

Based on the Knudsen number (Kn) and its range, three different types of flow mechanism (i.e. molecular diffusion, Knudsen mechanism, and transition process or Knudsen-molecular diffusion) can occur inside the DCMD module [32].

The membrane refinement coefficient (C_m) for Knudsen, molecular diffusion Knudsen-molecular diffusion flow mechanism can be obtained from Ref. [37]:

$$C_m = \frac{2}{3}\frac{\varepsilon r}{\tau \delta}\left(\frac{8M}{\pi RT}\right)^{0.5} \tag{20}$$

$$C_m = \frac{\varepsilon r}{\tau \delta}\frac{PD}{P_a}\frac{M}{RT} \tag{21}$$

$$C_m = \left[\frac{2}{3}\frac{\varepsilon r}{\tau \delta}\left(\frac{8M}{\pi RT}\right)^{0.5} + \frac{\varepsilon r}{\tau \delta}\frac{PD}{P_a}\frac{M}{RT}\right] \tag{22}$$

At the beginning of the iterative computer modelling, $T_{f,m}$ and $T_{p,m}$ are assumed to be equal to the feed and product streams bulk temperatures (i.e. T_{bf} and T_{bp}), respectively. The following equations are used to determine the new values of $T_{f,m}$ and $T_{p,m.}$ respectively. The process is repeated by a number of iterations until $T_{f,m}$ and $T_{p,m}$ reach the acceptable precision.

$$T_{f,m} = \frac{h_m\left(T_p + \left(\frac{h_p}{h_f}\right)T_f\right) + h_f T_f + J_w H_v}{h_m + h_f\left(1 + \frac{h_m}{h_p}\right)} \tag{23}$$

$$T_{p,m} = \frac{h_m\left(T_f + \left(\frac{h_p}{h_f}\right)T_p\right) + h_p T_p + J_w H_v}{h_m + h_p\left(1 + \frac{h_m}{h_f}\right)} \tag{24}$$

3.2. Multi-step calculation process for membrane desalination system

A sub-program was developed to simulate the performance of DCMD modules. This computation process is a part of the overall computation process designed to simulate the performance of the whole system.

In order to specify the temperature and salinity changes along the DCMD module, Equations (7–24) were solved for a single section. Then, Eqs. (1)–(6), which are the mass and energy balance equations, were solved to determine the input boundary conditions of the next section.

Outlet salinity and temperature are the unknown parameters of the combination of Eqs. (3) and (4). To obtain an additional equation to remove one of these unknowns, the following equation which is the salt mass balance equation was used. Numerical methods (e.g., Secant Method) were used to solve Eq. (25) as it is not related to the outlet temperature linearly.

$$\frac{m_{f,n}}{\rho_{f,n}} S_{f,n} = \frac{m_{f,n+1}}{\rho_{f,n+1}} S_{f,n+1} \tag{25}$$

The computation process begins with initial guesses of cold stream outlet temperature (T_a) as well as mass transfer through the DCMD module (J_{wa}). The following boundary conditions applied in the computer modelling. The next step is calculating the cold flow inlet temperature and comparing the obtained value with the actual one. The initial guess should change if the obtained difference is not within the acceptable error range (i.e. 0.0001 °C). The same process was applied and repeated for the cold flow inlet flow rate.

$$m_w = \sum_{n=1}^{n=j} J_{w,n} A_{m,n} \tag{26}$$

$$T_{f,0} = T_{f,in} \tag{27}$$

$$T_{f,j} = T_{f,out} \tag{28}$$

$$T_{d,0} = T_{f,in} - T_a \tag{29}$$

$$T_{d,j} = T_{d,in} \tag{30}$$

$$S_{f,0} = S_{f,in} \tag{31}$$

$$S_{f,j} = S_{f,out} \tag{32}$$

$$S_{p,0} = 0 \tag{33}$$

$$S_{p,j} = 0 \tag{34}$$

$$m_{p,0} = m_{p,in} + \sum_{n=1}^{j} J_{wa,n} A_{m,n} \tag{35}$$

3.3. Mixed effect absorption cooling unit

The Following assumptions are considered for the simulation of the mixed absorption refrigeration system [38,39]: (i) all processes happen in steady state; (ii) the pressure drop in connecting lines is neglected; (iii) the output vapour from the HP generator reaches saturated liquid state after transmitting its heat to the solution that exists inside the LP generator; (iv) flow inside pump and expansion valve is isenthalpic; (v) the refrigerant leaves the evaporator and the condenser in saturated state; (vi) the pressure difference between the condenser and the LP generator is low.

In each section of the absorption refrigeration system, there is an inlet and outlet flow. Equilibrium of mass, concentration, and energy for each section of the cooling system in steady state situation is as follows.

$$\sum m_i = \sum m_o \tag{36}$$

$$\sum m_i \omega_i = \sum m_o \omega_o \tag{37}$$

$$\sum m_i h_i - \sum m_o h_o = Q \tag{38}$$

It is vital to obtain the characteristics of the LiBr/water solution. To do so, the thermodynamic formulations proposed in the literature are used [40]. The formulation is derived from empirical records and is presented based on some parameters such as molar ratio and temperature.

$$C_p(T,x) = (1-x)C_p'(T) + C_{p,t}\sum_{i=1}^{8} a_i x^{m_i}(0.4-x)^{n_i}\left(\frac{T_c}{T-T_0}\right)^{t_i} \tag{39}$$

$$h(T,x) = (1-x)h'(T) + h_c\sum_{i=1}^{30} a_i x^{m_i}(0.4-x)^{n_i}\left(\frac{T_c}{T-T_0}\right)^{t_i} \tag{40}$$

h'(T) and C′(p) represent the characteristics of the saturated water in liquid state.

$$P(T,x) = P_\sigma(\theta) \tag{41}$$

$$\theta = T - \sum_{i=1}^{8} a_i x^{m_i}(0.4-x)^{n_i}\left(\frac{T}{T_c}\right)^{t_i} \tag{42}$$

In the abovementioned equations, the pressure of the solution at hypothetical temperature θ is equivalent to liquid saturation pressure.

Following equation is also applied to relate the mass ratio to the molar ratio of water-lithium bromide solution:

$$\omega = \frac{xM_{LiBr}}{xM_{LiBr} + (1-x)M_w} \tag{43}$$

Precise water data in both saturated and liquid states are also necessary for a correct simulation. These properties are extracted from REFPROP software and the required data in super-heated state are calculated by the formulas proposed by Lachkov et al. [41]. The expressions for the calculation of enthalpy, viscosity, and superheated vapour density have been obtained under different operating conditions and within the actual piping.

For the components that have inlet and outlet fluid, the following equation can be applied to calculate the transferred heat [42]:

$$Q = mC_p(T_o - T_i) \tag{44}$$

As mentioned earlier, the lower section of the LP generator receives its required heat from condensation of refrigerant vapour that comes from the high pressure generator. This heat can be obtained by using the following equation:

$$Q = m(h_o - h_i) \tag{45}$$

where m (kg/s) is the mass flow rate, and h_i and h_o (kj/kg) are the inlet and the outlet enthalpy, respectively.

Logarithmic mean temperature difference is applied to each section to calculate the temperature difference.

$$\Delta T_{LMTD} = \frac{(T_{i,1} - T_{o,2}) - (T_{o,1} - T_{i,2})}{Ln\left[(T_{i,1} - T_{o,2})/(T_{o,1} - T_{i,2})\right]} \tag{46}$$

and

$$Q = UA\Delta T_{LMTD} \tag{47}$$

Mixed effect absorption chiller's coefficient of performance is obtained from:

$$COP = \frac{Q_e}{Q_{ex} + Q_{jw} + W_p} \tag{48}$$

As explained previously, a finned-tube heat exchanger is implemented to extract the available heat from the diesel exhaust and to transmit it to water. The actual mode of the heat exchanger is a cross flow arrangement, but due to enough number of rows, the flow mechanism inside the heat exchanger can be evaluated as counter flow. To achieve the optimum performance, diesel exhaust is assumed to be in the exterior section and the following equation is applied to calculate heat transfer coefficient [43].

$$h_{ex} = 0.1378\frac{k_{ex}}{d_o}\left(\frac{d_o m_{ex}}{\mu_{ex} A}\right)^{0.718} Pr_{ex}{}^{1/3}\left(\frac{s}{\delta}\right)^{0.296} \tag{49}$$

In order to better evaluate heat transfer efficiency, a parameter called heat transfer ratio (HC) was considered. This parameter is the heat transfer coefficient of the HP divided by the evaporator heat transfer coefficient. Among all the heat transfer processes, heat transfer inside HPG and evaporator are the most important ones. This is mainly because exhaust gases, which are the main powering source of the system, transfer heat inside HPG and heat transfer inside evaporator directly affects the overall output of the system. Therefore, the heat transfer ratio relates these two heat transfer processes which are functions of physical and operational parameters of the system.

$$HC = \frac{UA_{HPg}}{UA_{eva}} \tag{50}$$

The general process of the simulation is illustrated in Fig. A-1 in the appendix section. To have a theoretical model with a reasonable computational expense, instead of analysing the performance of side systems (i.e. the cooling water loops of absorption and desalination unit and also the refrigerant water loop), several assumptions are considered [44]. The inlet temperature and mass flow rate of refrigerant water (used for cooling and air conditioning) and cooling water (used in absorber and condenser) in absorption unit are set constant at 12 °C and 1.64 Kg/s and 25 °C and 3.36 kg/s, respectively. Also, it is assumed that the cooling water for the desalination system enters the membrane module at 25 °C [44].

Table 1 presents the characteristics of the membrane module, the heat exchanger under consideration for heating unit, and the engine. As the information of submarine engines are confidential, the authors used the available data for submarine engines provided

Table 1
The characteristics considered for the simulation.

Parameter	Value	Parameter	Value
DCMD module			
Membrane length	0.475 m	Nominal pore size	0.5 μm
Membrane width	0.235 m	Number of modules	10
Membrane thickness	210 μm	porosity	80%
Heat recovery HE			
Tube quantity	50	Pipe distance	54 mm
External radius	13.5 mm	Fin concentration	50
Internal radius	10 mm	Fin height	27 mm
Arrangement	Staggered	Fin thickness	4 mm
Tube length	40 cm	Fin material	Inox steel
Row distance	46 mm	Tube material	Inox steel
Diesel engine			
Model number	16–248	Number of cylinder	16
Bore	8.5	stroke	10.5
Rated engine speed	765 rpm	Type of engine	2 cycles
Cylinder arrangement	40° "V"	Starting system	Air

by General Motors company including the exhaust characteristics and load of the engine.

4. Results and discussion

The diesel exhaust mass flow rate is directly related to engine's operating conditions, hence, it is not reasonable to consider a constant value for it. On the other hand, the submarine engines' specifications including load curves are highly confidential. To overcome this issue, a parameter called "exhaust gas mass ratio (X)" is defined that is the ratio of the outlet exhaust mass flow rate to the maximum operational outlet mass flow rate. Fig. 3 shows the output temperature variations of the heating unit versus X, at various flow rates. This diagram can be used for increasing the accuracy of the design, performance prediction, and monitoring of the heating unit. For instance, the results show that the water temperature reaches 60 °C when the water mass flow rate is 0.24 kg/s and X = 0.3. The same temperature can be achieved with a water mass flow rate of 0.3 kg/s and X = 0.4 or with a water mass flow rate of 0.36 kg/s and X = 0.5. The analysis diagram shows that at different water mass flow rates, the outlet water temperature increases as X increases. Also, by having a constant X, reducing the mass flow rate of the water increases the output temperature of the heat exchanger. This is particularly noticeable at high X values. For example, as the mass flow rate that enters the heat exchanger at X = 0.25 decreases by 50%, the water temperature increases by 18 °C. This increase is about 26 °C at X = 0.45. The results clearly indicate that the outlet temperature of the heat exchanger and consequently the freshwater productivity of the desalination unit are functions of both exhaust gas mass ratio and water mass flow rate.

4.1. Water productivity

Fig. 4 depicts the changes in the mass flux of the membrane versus X, for water mass flow rates of 0.2–0.4 kg/s. By increasing X at a constant water mass flow rate, the water temperature inside the hot channel rises. Consequently, the temperature gradient between the hot and cold sides of the membrane and the driving force of the mass flux through the module increases leading to higher vapour mass

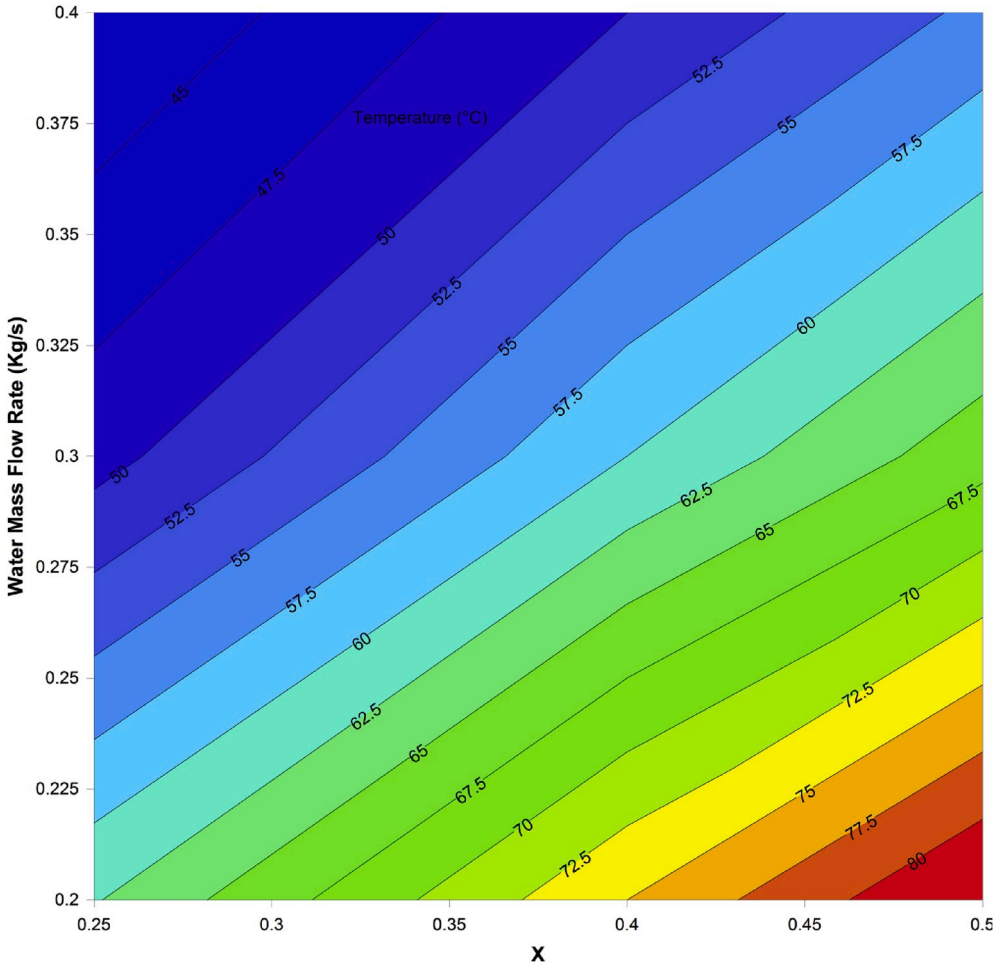

Fig. 3. The output temperature variations of the heating unit versus X, at various flow rates.

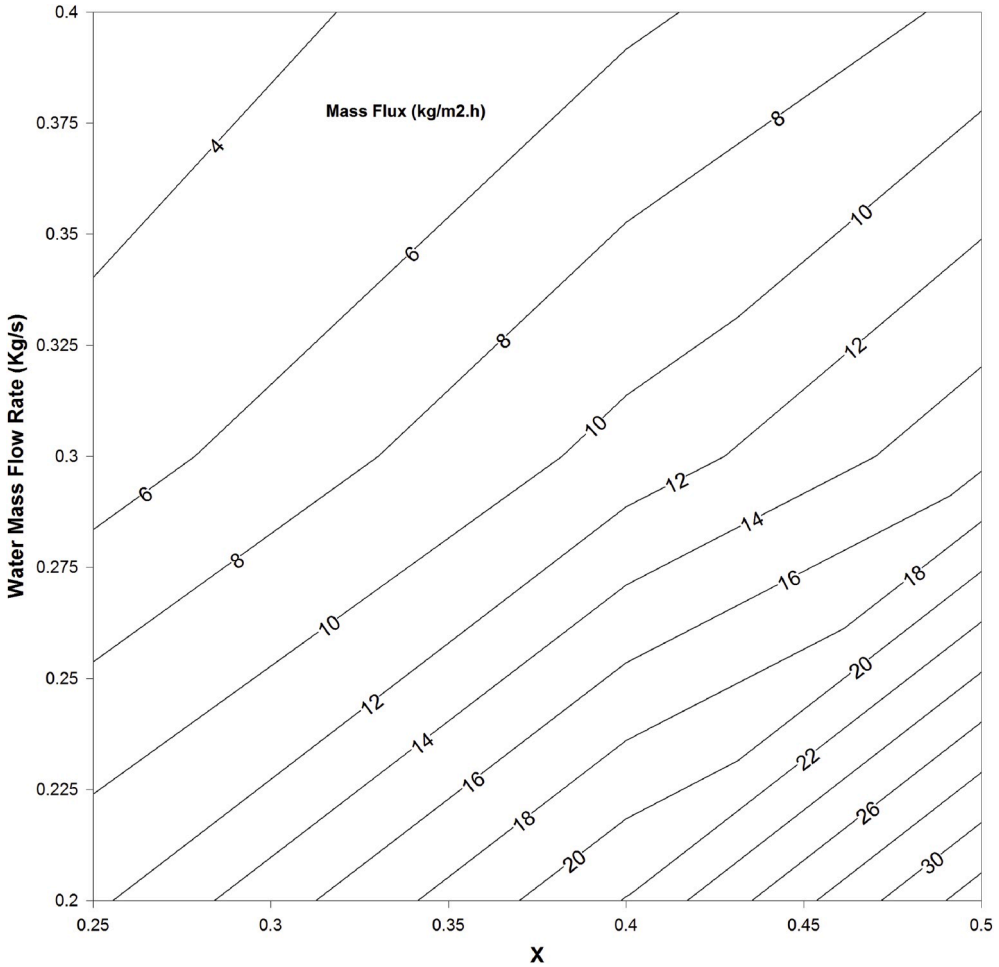

Fig. 4. Mass transfer through the membrane versus X at various mass flow rates.

flux through the membrane. For instance, the mass flux through the membrane reaches 4 kg/m^{2}h when the water mass flow rate is 0.35 kg/s and X = 0.27. This number is about 8 kg/m^{2}h for X = 0.4 and 10 kg/m^{2}h for X = 0.48. The results in this figure show that the rate of mass flux increases with increasing X and decreasing the mass flow rate. For example, when the water mass flow rate is 0.25 kg/s, increasing X from 0.25 to 0.3 results in a 2 kg/m^{2}h increase in membrane mass flux. At the same water mass flow rate, as X rises from 0.45 to 0.5, the mass flux of the membrane increases by 5 kg/m^{2}h.

It should be noted that both water temperature and mass flow rate inside the hot channels are important parameters in calculating the mass transfer through the membrane. The results in Fig. 4 shows that in this system, where both parameters are variable, the effect of the temperature is higher than the effect of mass flow rate. Reducing the mass flow rate increases the water temperature that comes out of the heat exchanger. Consequently, the temperature difference which exists between two sides of the membrane increases. However, when feed water temperature is constant, increasing the water mass rate will increase the amount of fresh water productivity. Increasing the temperature difference between the membrane and the streams lowers the thermal resistance inside the boundary layers. This increases the mass flux through the membrane since there is a direct relation between thermal resistance and membrane surface temperature difference, and hence, vapour pressure difference that is the main driving force of the process. Overall, one can conclude that the freshwater productivity of the desalination unit is more sensitive to the feed temperature than its mass flow rate. Therefore, if a specific amount of extra energy is available, it is recommended to be used to reach a higher temperature of seawater.

4.2. Cooling

The effect of X values on the refrigeration power at different refrigerant mass flow rates is shown in Fig. 5. This diagram helps to increase the accuracy of the design, performance prediction, and monitoring of an absorption refrigeration unit. The results indicate that a specific refrigeration power can be achieved when other parameters are within a certain range. For instance, a power of 160 kW can be reached when X is between 0.8 and 0.95 and the refrigerant mass flow is between 0.27 kg/s and 0.34 kg/s. It is apparent from the results that increasing these two parameters increases the refrigeration capacity. Consequently, at a refrigerant mass flow rate of 0.06 kg/s and X = 0.2, the refrigeration system reaches 118 kW. This can be increased to 160 kW at a refrigerant mass flow rate of 0.3

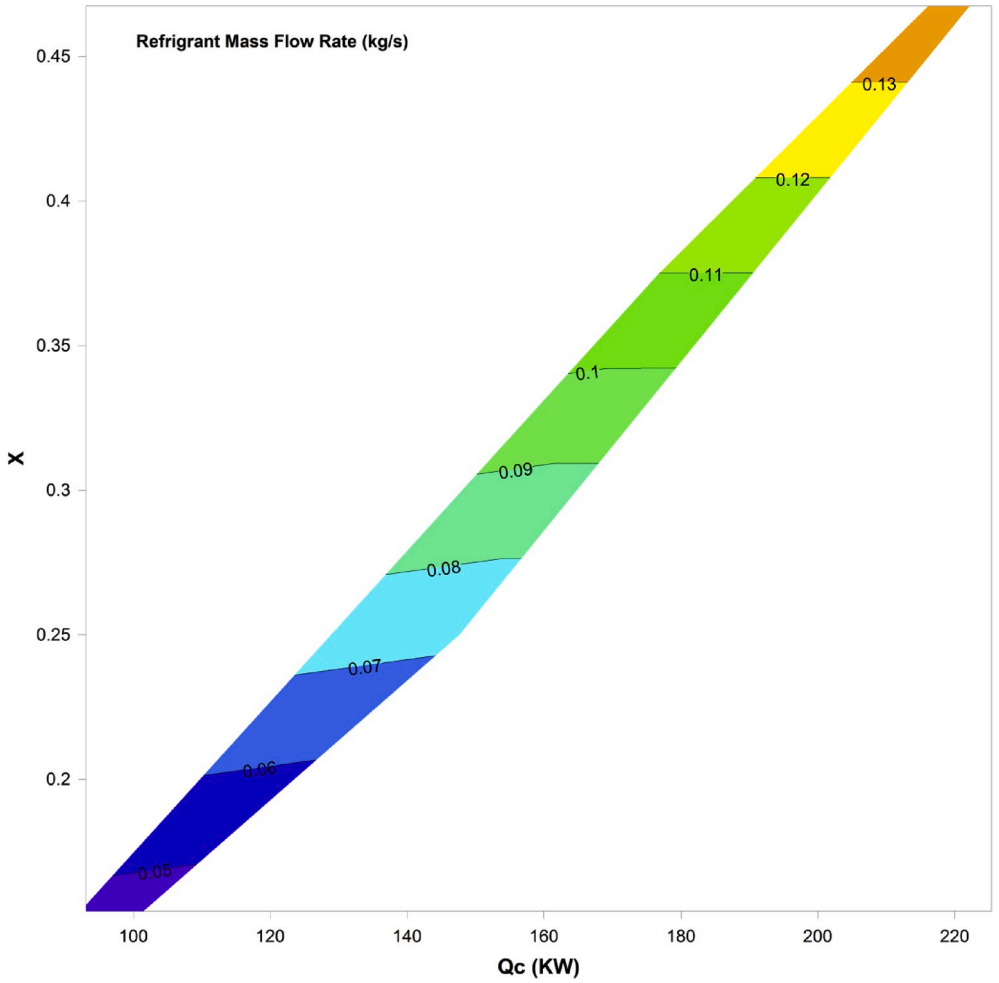

Fig. 5. The effect of X on the absorption refrigeration power at different refrigerant mass flow rates.

kg/s and X = 0.09. The middle power range, i.e. from 130 to 190 kW, occurs in a larger area of the functional parameters, while the lower or higher powers have smaller areas.

Fig. 6 presents the effect of the heat transfer coefficient on the COP of the mixed absorption refrigeration system in terms of X. The results clearly show that the performance coefficient rises as the heat transfer coefficient and X increase. Also, in a constant exhaust mass flow ratio, raising the heat transfer coefficient improves the COP of the absorption refrigeration unit. It is worth noting that the heat transfer coefficient and X are correlated where a change in one parameter needs to take place within a specified range of the other one. For instance, the heat transfer coefficient of 0.45 can be used only when the exhaust gas mass ratio is between 0.37 and 0.53, which yields a COP within the range 0.83–0.88. Overall, the COP of the cooling system can be concluded to be a function of energy source (i.e. exhaust mass ratio) as well as operational and physical characteristics of the refrigeration system.

Fig. 7 illustrates changes in the refrigeration temperature versus X values at different refrigerant mass rates. The trend for the refrigeration temperature falls upon increasing X and the refrigerant mass rate. At a refrigerant mass rate of 0.06 kg/s and X = 0.2, the refrigeration temperature is about 6 °C while it falls to 4 °C as these parameters increase to 0.1 kg/s and 0.34, respectively. This figure shows that a lower outlet refrigeration temperature results in the system having a higher cooling power. This is due to the fact that there is a direct correlation between the refrigeration temperature and the cooling capacity of the system.

4.3. Heat recovery

Fig. 8 depicts the overall percentage of the recovered heat versus X, at various flow rates. The analysis diagram indicates that at different water mass flow rates, the trend for the overall percentage of the recovered heat increases as X increases. For instance, at water mass flow rate of 0.2 Kg/s, the percentage of the recovered heat is ~70.5% for X = 0.275 while this value is 81% for X = 0.5. Moreover, by having a constant X, increasing the mass flow rate of the water increases the amount of recovered heat.

Overall, applying this system in submarines can reduce fossil fuel consumption resulting in many positive environmental and economic consequences. The built-in desalination system can reduce the dependency to the cosmetic potable water resources and more

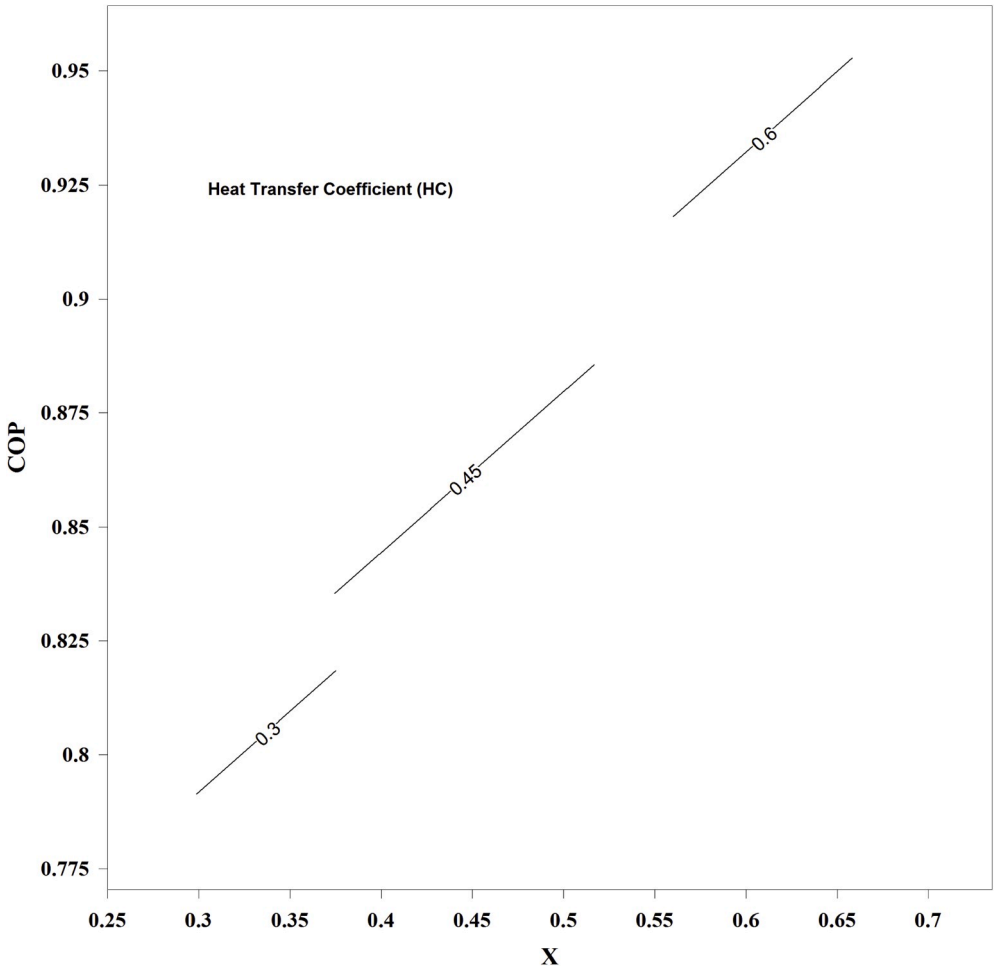

Fig. 6. Effect of heat transfer coefficient on COP of the mixed absorption refrigeration unit in terms of X.

water can be conserved. Also, submarines do not have to carry all the required water for their operation anymore and their weight decreases. Subsequently, submarines need less driving power and can stay underwater for longer time.

5. Conclusions

The present study proposes a novel combined desalination, cooling, and air-conditioning system to recover and apply the waste heat from engine exhaust gas and water jacket of submarine diesels. The findings of this study can be summarised as follows:

- The effect of water temperature on the mass flux through the membrane is higher than hot water mass flow rate, therefore, higher mass fluxes can be achieved at higher exhaust gas mass ratios and lower mass flow rates.
- A specific refrigeration power can be achieved when other parameters (i.e. X values and refrigerant mass flow rate) are within a certain range. The power range of 130–190 kW is achievable within a larger area of the functional parameters, while for the lower or higher power ranges, the variability of these parameters are limited.
- Coefficient of performance (COP) within the range of 0.83–0.88 can be achieved when the heat transfer coefficient is 0.45 and the exhaust gas mass ratio is between 0.37 and 0.53.
- The proposed system reduces the consumption of fossil fuels and also removes the necessity of outsourcing fresh water in submarines. Consequently, the weight of submarines decreases and less driving power is required.

CRediT authorship contribution statement

Abdellah Shafieian: Investigation, Methodology, Formal analysis, Visualization, Writing - original draft. **Mehdi Khiadani:** Supervision, Conceptualization, Writing - review & editing.

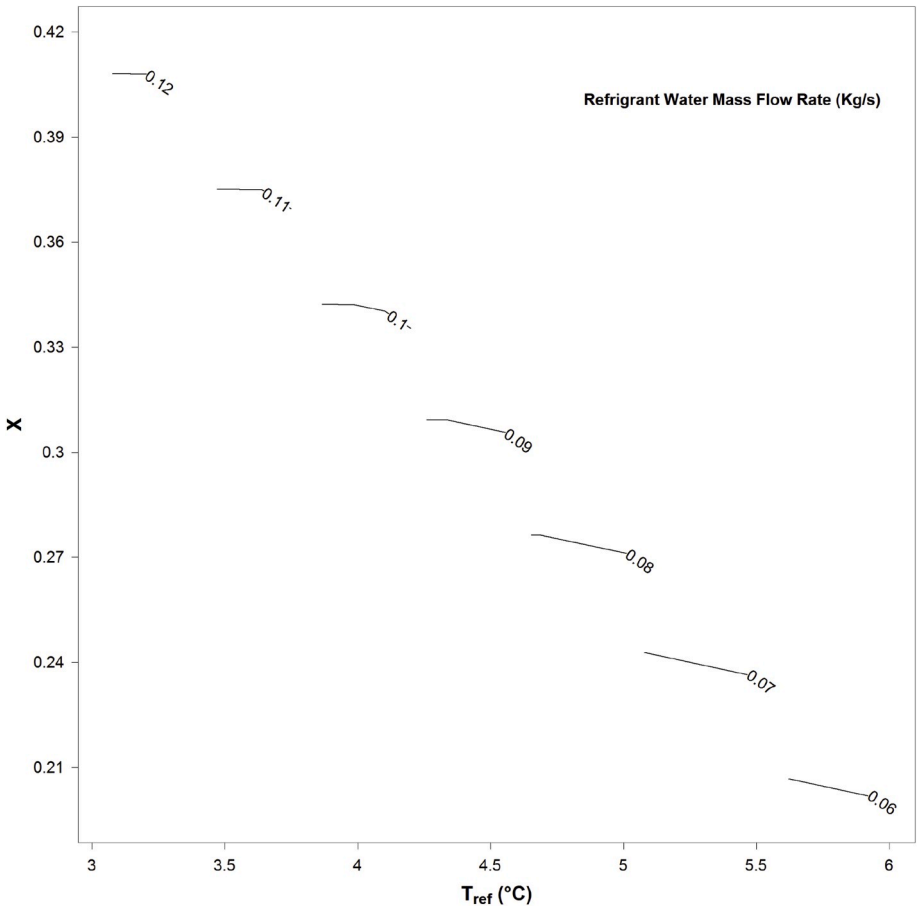

Fig. 7. Changes in refrigeration temperature versus X at different refrigerant mass rates.

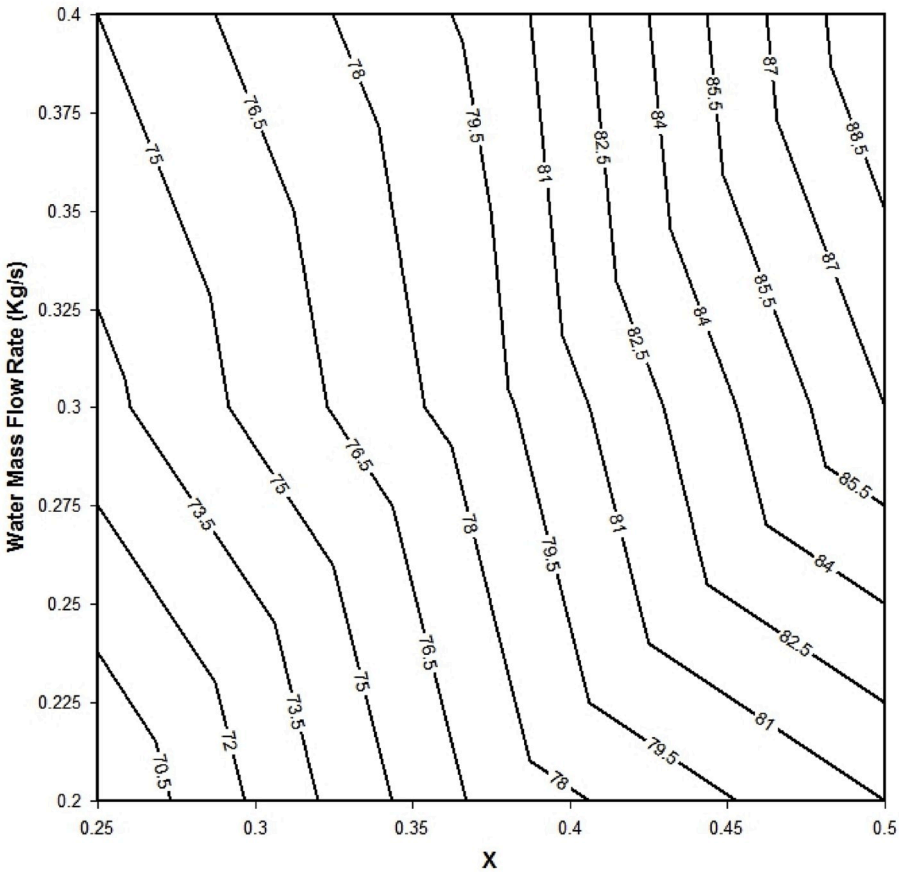

Fig. 8. The overall percentage of recovered heat versus X, at various flow rates.

Appendix

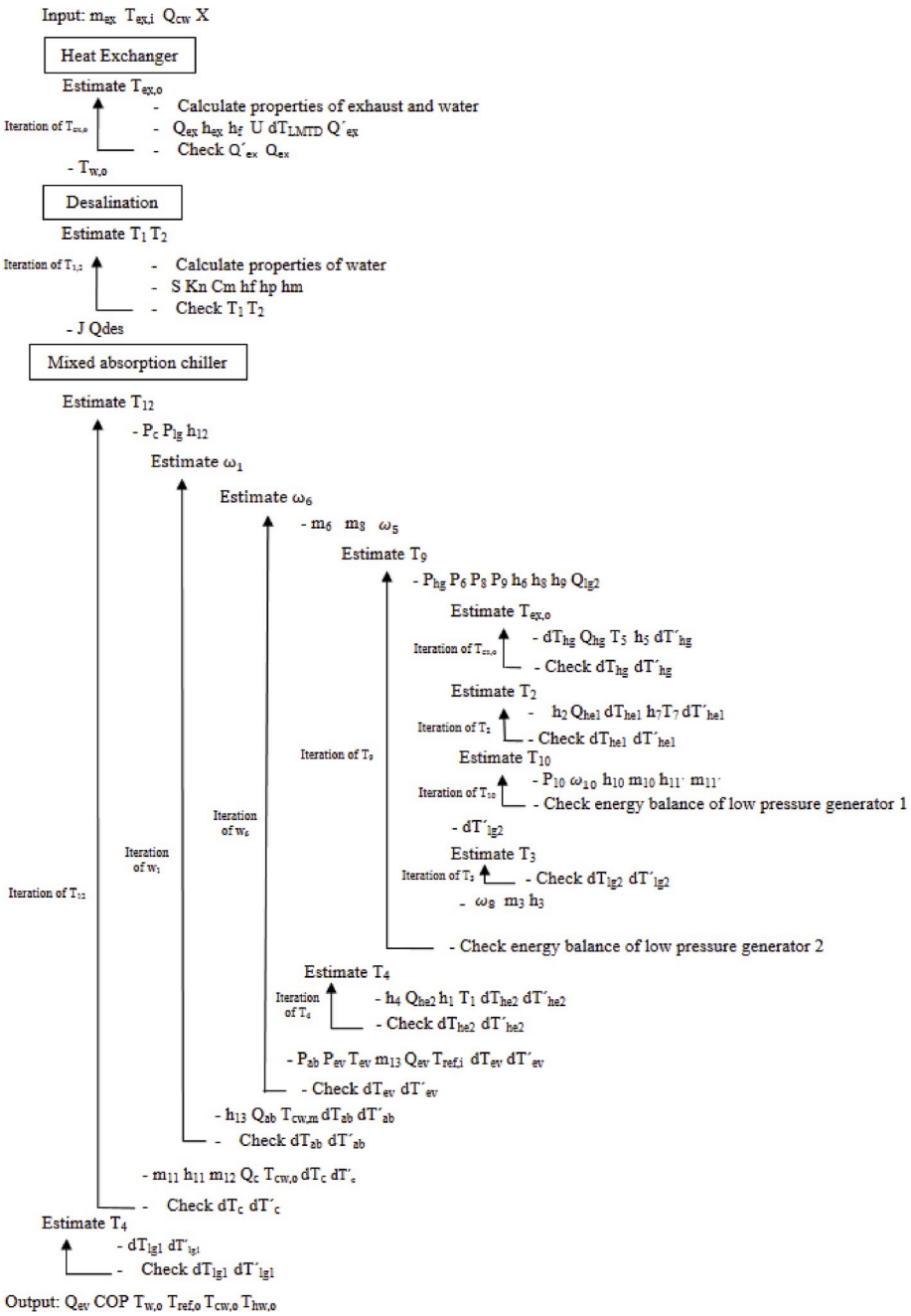

Fig. A-1. The simulation flowchart of the whole system.

Appendix A. Supplementary data

Supplementary data to this article can be found online at https://doi.org/10.1016/j.csite.2020.100702.

References

[1] Submarine Emergency Diesel Engine Wet Exhaust: Nature of Discharge, Phase I Final Rule and Technical Development Document of Uniform National Discharge Standards (UNDS). United States: United States Environmental Protection Agency, 1999. Reference number EPA-842-R-99-001.
[2] M. Erguvan, D.W. MacPhee, Second law optimization of heat exchangers in waste heat recovery, Int. J. Energy Res. 43 (2019) 5714–5734.
[3] T. Chen, G. Shu, H. Tian, X. Ma, Y. Wang, H. Yang, Compact potential of exhaust heat exchangers for engine waste heat recovery using metal foams, Int. J. Energy Res. 43 (2019) 1428–1443.
[4] B. Xu, D. Rathod, S. Kulkarni, A. Yebi, Z. Filipi, S. Onori, Transient dynamic modeling and validation of an organic Rankine cycle waste heat recovery system for heavy duty diesel engine applications, Appl. Energy 205 (2017) 260–279.
[5] H. Koppauer, W. Kemmetmüller, A. Kugi, Modeling and optimal steady-state operating points of an ORC waste heat recovery system for diesel engines, Appl. Energy 206 (2017) 329–345.
[6] S. Seyedkavoosi, S. Javan, K. Kota, Exergy-based optimization of an organic Rankine cycle (ORC) for waste heat recovery from an internal combustion engine (ICE), Appl. Therm. Eng. 126 (2017) 447–457.
[7] F. Yang, H. Cho, H. Zhang, J. Zhang, Thermoeconomic multi-objective optimization of a dual loop organic Rankine cycle (ORC) for CNG engine waste heat recovery, Appl. Energy 205 (2017) 1100–1118.
[8] V. Chintala, S. Kumar, J.K. Pandey, A technical review on waste heat recovery from compression ignition engines using organic Rankine cycle, Renew. Sustain. Energy Rev. 81 (2018) 493–509.
[9] S. Lion, C.N. Michos, I. Vlaskos, C. Rouaud, R. Taccani, A review of waste heat recovery and Organic Rankine Cycles (ORC) in on-off highway vehicle Heavy Duty Diesel Engine applications, Renew. Sustain. Energy Rev. 79 (2017) 691–708.
[10] S. Lan, Z. Yang, R. Chen, R. Stobart, A dynamic model for thermoelectric generator applied to vehicle waste heat recovery, Appl. Energy 210 (2018) 327–338.
[11] A. Goyal, M.A. Staedter, D.C. Hoysall, M.J. Ponkala, S. Garimella, Experimental evaluation of a small-capacity, waste-heat driven ammonia-water absorption chiller, Int. J. Refrig. 79 (2017) 89–100.
[12] X. Liu, M.Q. Nguyen, M. He, Performance analysis and optimization of an electricity-cooling cogeneration system for waste heat recovery of marine engine, Energy Convers. Manag. 214 (2020), 112887.
[13] X. Liu, M.Q. Nguyen, J. Chu, T. Lan, M. He, A novel waste heat recovery system combing steam Rankine cycle and organic Rankine cycle for marine engine, J. Clean. Prod. (2020), 121502.
[14] S. Lion, I. Vlaskos, R. Taccani, A review of emissions reduction technologies for low and medium speed marine Diesel engines and their potential for waste heat recovery, Energy Convers. Manag. 207 (2020), 112553.
[15] Y. Liang, Z. Sun, M. Dong, J. Lu, Z. Yu, Investigation of a refrigeration system based on combined supercritical CO2 power and transcritical CO2 refrigeration cycles by waste heat recovery of engine, Int. J. Refrig. (2020). In press.
[16] A.G. Mohammed, M. Mosleh, W.M. El-Maghlany, N.R. Ammar, Performance analysis of supercritical ORC utilizing marine diesel engine waste heat recovery, Alexandria Eng. J. 59 (2020) 893–904.
[17] Z. Su, T. Ouyang, J. Chen, P. Xu, J. Tan, N. Chen, et al., Green and efficient configuration of integrated waste heat and cold energy recovery for marine natural gas/diesel dual-fuel engine, Energy Convers. Manag. 209 (2020) 112650.
[18] S. Zhu, K. Zhang, K. Deng, A review of waste heat recovery from the marine engine with highly efficient bottoming power cycles, Renew. Sustain. Energy Rev. 120 (2020), 109611.
[19] A.N. Eddine, D. Chalet, X. Faure, L. Aixala, P. Chessé, Optimization and characterization of a thermoelectric generator prototype for marine engine application, Energy 143 (2018) 682–695.
[20] X. Xu, Y. Li, S. Yang, G. Chen, A review of fishing vessel refrigeration systems driven by exhaust heat from engines, Appl. Energy 203 (2017) 657–676.
[21] T. Ouyang, Z. Su, B. Gao, M. Pan, N. Chen, H. Huang, Design and modeling of marine diesel engine multistage waste heat recovery system integrated with flue-gas desulfurization, Energy Convers. Manag. 196 (2019) 1353–1368.
[22] M. Hatami, D. Ganji, M. Gorji-Bandpy, Numerical study of finned type heat exchangers for ICEs exhaust waste heat recovery, Case Studies Ther. Eng. 4 (2014) 53–64.
[23] H. Jaber, M. Khaled, T. Lemenand, M. Ramadan, Effect of generator load on hybrid heat recovery system, Case Studies Ther. Eng. 13 (2019), 100359.
[24] R. Daghigh, A. Shafieian, An investigation of heat recovery of submarine diesel engines for combined cooling, heating and power systems, Energy Convers. Manag. 108 (2016) 50–59.
[25] E. Kurem, I. Horuz, A comparison between ammonia-water and water-lithium bromide solutions in absorption heat transformers, Int. Commun. Heat Mass Tran. 28 (2001) 427–438.
[26] A. Shafieian, M. Khiadani, A. Nosrati, Performance analysis of a thermal-driven tubular direct contact membrane distillation system, Appl. Therm. Eng. (2019), 113887.
[27] K. Nakoa, K. Rahaoui, A. Date, A. Akbarzadeh, Sustainable zero liquid discharge desalination (SZLDD), Sol. Energy 135 (2016) 337–347.
[28] A. Shafieian, M. Khiadani, A novel solar-driven direct contact membrane-based water desalination system, Energy Convers. Manag. 199 (2019), 112055.
[29] M. Macklin, Air Conditioning Systems Study for Nuclear Powered Submarines, Annual meeting of the Society of Naval Architects and Marine Engineers, 1961.
[30] R.D. Gustafson, J.R. Murphy, A. Achilli, A stepwise model of direct contact membrane distillation for application to large-scale systems: experimental results and model predictions, Desalination 378 (2016) 14–27.
[31] M.H. Sharqawy, J.H. Lienhard, S.M. Zubair, Thermophysical Properties of Seawater: a Review of Existing Correlations and Data vol. 16, Desalin Water Treat, 2010, pp. 354–380.
[32] A. Alkhudhiri, N. Darwish, N. Hilal, Membrane distillation: a comprehensive review, Desalination 287 (2012) 2–18.
[33] Y. Yun, R. Ma, W. Zhang, A.G. Fane, J. Li, Direct contact membrane distillation mechanism for high concentration NaCl solutions, Desalination 188 (2006) 251–262.
[34] U.L. Dahiru, E.K. Atia, Theoretical and statistical models for predicting flux in direct contact membrane distillation, J. Eng. Res. Appl. 4 (2014) 124–135.
[35] A.M. Elzahaby, A.E. Kabeel, M.M. Bassuoni, A.R.A. Elbar, Direct contact membrane water distillation assisted with solar energy, Energy Convers. Manag. 110 (2016) 397–406.
[36] K. Nakoa, K. Rahaoui, A. Date, A. Akbarzadeh, Sustainable zero liquid discharge desalination (SZLDD), Sol. Energy 136 (2016) 337–347.
[37] M.R. Qtaishat, F. Banat, Desalination by solar powered membrane distillation systems, Desalination 308 (2013) 186–197.
[38] Z. Xu, R. Wang, Z. Xia, A novel variable effect LiBr-water absorption refrigeration cycle, Energy 60 (2013) 457–463.
[39] R. Gomri, Simulation study on the performance of solar/natural gas absorption cooling chillers, Energy Convers. Manag. 65 (2013) 675–681.
[40] J. Patek, J. Klomfar, A computationally effective formulation of the thermodynamic properties of LiBr–H2O solutions from 273 to 500 K over full composition range, Int. J. Refrig. 29 (2006) 566–578.
[41] V. Lachkov, A. Lysenkov, Y.V. Mamonov, Expressions for thermophysical properties of superheated steam, Meas. Tech. 42 (1999) 58–60.
[42] R. Daghigh, A. Shafieian, Energy and exergy evaluation of an integrated solar heat pipe wall system for space heating, Sādhanā 41 (2016) 877–886.
[43] W.Z. Gu, J.R. Shen, C.F. Ma, Y.M. Zhang, Enhanced Heat Transfer, Science Press, Beijing, 1990 ([in Chinese]).
[44] J. Wang, J. Wu, Investigation of a mixed effect absorption chiller powered by jacket water and exhaust gas waste heat of internal combustion engine, Int. J. Refrig. 50 (2015) 193–206.